3D XY and Lowest Landau Level Fluctuations in Deoxygenated $YBa_2Cu_3O_{7-\delta}$ Thin Films

Katerina Moloni, Mark Friesen, Shi Li, Victor Souw, P. Metcalf, Lifang Hou, and M. McElfresh

Physics Department, Purdue University, West Lafayette, Indiana 47907-1396

(Received 22 August 1996; revised manuscript received 5 November 1996)

Conductivity measurements reflect vortex solid melting in $YBa_2Cu_3O_{7-\delta}$ films. Field-independent glass exponents $\nu_g \simeq 1.9$ and $z_g \simeq 4.0$ describe the transition $T_g(H)$ for $0 < H \leq 26$ T. At low fields, 3D XY exponents $\nu_{XY} \simeq 0.63$ and $z_{XY} \simeq 1.25$ are also observed, with z_{XY} smaller than expected. These compete with glass scaling according to multicritical theory. A predicted power-law form of $T_g(H)$ is observed for $0.5T_c < T_g < T_c$. For $T_g < 0.5T_c$, 3D XY scaling fails, but a self-consistent lowest Landau level analysis becomes possible, obtaining $T_{c2}(H)$ with positive curvature. [S0031-9007(97)02912-8]

PACS numbers: 74.25.Bt, 74.25.Dw, 74.40.+k, 74.72.–h

The nature of fluctuations near the superconducting to normal state transition in high-temperature superconductors (HTSCs) is still a matter of controversy. Several distinct fluctuation types and regions have been proposed, e.g., 3D XY fluctuations at low fields, lowest Landau level (LLL) fluctuations at high fields, and glasslike fluctuations (for disordered HTSCs) near the finite-field transition $T_g(H)$. However, experimental analyses based upon the different scaling theories lead to conflicting results. This situation is most evident for competing 3D XY and LLL fluctuations, *both* of which are supported experimentally, in the same region of the phase diagram, in spite of being incompatible [1].

The 3D XY transition is driven by phase fluctuations of a complex order parameter (OP) which fall into the universality class of the λ transition in ^{4}He. The zero-field, "intermediate" (nonelectrodynamic) phase fluctuations of the HTSCs are thought to be of this type [2]. At $T = T_c$ (and $H = 0$), these fluctuations diverge in size, driving the resistive phase transition. Recent experimental evidence supporting this picture is found in specific heat [3,4], magnetization [4,5], penetration depth [6], and current-voltage (J-E) measurements [4,7]. The finite-field transition $T_g(H)$, which is similarly driven by phase fluctuations of the OP, joins smoothly to $T_c \equiv T_g(H = 0)$. However, the glass and 3D XY fluctuations exhibit distinct scaling functions and exponents [2].

Fluctuations of the OP *amplitude* occur near the upper critical (mean-field) temperature $T_{c2}(H)$. These fluctuations drive the Cooper pair density to zero, but do not correspond to a true transition; superconducting order vanishes at the slightly lower temperature $T_g(H)$. In the low-field region, the distinction between OP amplitude and phase fluctuations results in the dominance of 3D XY critical behavior near $T = T_c$. At high fields, this distinction is not present, yielding a different type of behavior, most conveniently described in terms of the Ginzburg-Landau LLL approximation, with its corresponding scaling theory [8,9]. Experimental evidence in support of this behavior is found in specific heat [10–12], magnetization [10,12], and J-E characteristics [10,13]. A crossover is expected between the low-field (3D XY) and high-field (LLL) behaviors, and its clarification is fundamental in the investigation of HTSC fluctuations [14].

It may appear that glass fluctuations near $T_g(H)$ only complicate the story, since they compete with both the low- and high-field fluctuations. However, in this Letter we suggest, to the contrary, that glass fluctuations *help* to identify low- and high-field behaviors, through the use of multicritical scaling theory. Such theories are applicable when fluctuations of different types compete for dominance. For example, in the low-field limit, $T_g(H)$ *joins* $T_c \equiv T_g(H = 0)$, forcing the distinct fluctuation types to coexist near the multicritical point T_c [2]. In this paper, multicritical predictions augment the 3D XY and LLL theories, thus clarifying their applicability to HTSCs.

To address these issues, it is desirable to work in both the low- and high-field regions of the phase diagram. In $YBa_2Cu_3O_{7-\delta}$ samples, $H_{c2}(0)$ is very large ($\gtrsim$100 T) for "optimal" ($\delta \simeq 0.05$) stoichiometry. We therefore focus on deoxygenated films, for which magnetic field scales are relatively small, allowing $H_{c2}(T)$ to be accessed over a wide temperature range. Three optimal c-axis $YBa_2Cu_3O_{7-\delta}$ films, approximately 4000 Å thick, were prepared, and then deoxygenated, as described elsewhere [15]. Films with resulting stoichiometries of $\delta \simeq 0.24$, 0.57, and 0.59 (± 0.05) were produced, corresponding to T_c of 77, 61, and 56 K, respectively. The films were patterned into 100×2000 μm bridges using laser ablation. Isothermal J-E and conductivity (σ) curves were obtained using a conventional four-point geometry. As typical for underdoped samples, the normal state contribution could not be eliminated from σ, as it is not yet well characterized. However, this background contribution should not affect the present results greatly, in the temperature range of interest, due to the insulating nature of the normal state. Magnetic fields were applied perpendicular to the film surface (parallel to the c axis) in the range $0 < H \leq 26$ T.

Transition temperatures T_g, corresponding to the continuous vortex solid melting transition, were deduced at

each applied field using the scaling ansatz of Fisher, Fisher, and Huse (FFH) [2]. (Note that this ansatz is isomorphic with any two-exponent scaling theory of the melting transition.) The appropriately scaled conductivity is given by $(J/E)\,|T - T_g|^{\nu_g(z_g-1)}$, while the scaled current is $(J/T)\,|T - T_g|^{-2\nu_g}$. Here, ν_g and z_g are the static and dynamic glass scaling exponents, respectively. The $H_g(T)$ phase boundaries determined in this way are shown in Fig. 1. The obtained scaling exponents are independent of δ [15] and H, with values of $\nu_g = 1.8-1.95$ and $z_g = 4.0-4.1$. This is consistent with the notion of a single, 3D, glass universality class.

As a first application of multicritical scaling, we note that the form of $H_g(T)$ [the inverse of $T_g(H)$] is specified at low fields by the 3D XY theory [2,4]: $H_g(T) = H^*(1 - T/T_c)^{2\nu_{XY}}$, where ν_{XY} ($\neq \nu_g$) is the 3D XY static exponent. The phase boundaries satisfy this relation over a wide temperature range, $0.5T_c \leq T \leq T_c$, as shown in Fig. 1 (inset), identifying the crossover temperature $T_b \simeq 0.5T_c$ as the limit of 3D XY scaling. The slope of these curves gives a (sample-averaged) exponent $\nu_{XY} = 0.63 \pm 0.04$, which compares favorably with the expected value of 0.669 [16]. This is then used to determine the sample-dependent field scale H^*. For the films used here, H^* is in the range 7–19 T, as compared to optimal samples for which H^* is on the order of 50 T. The crossover field $H_b \equiv H_g(T = T_b)$ was studied previously, and was suggested to separate 3D from 2D behavior along $H_g(T)$ [17,18]. However, the field independence of the glass transition does not corroborate this conclusion. Below, we demonstrate instead that, for fields $H < H_b$, the 3D XY description is in good agreement with the data while, for $H > H_b$, a self-consistent LLL description becomes possible.

It is possible to determine T_c at zero field using the FFH ansatz [2]. However, this procedure is known to become uncontrolled at very low fields, obtaining surprising results, such as nonuniversal exponents [19]. Therefore, we develop here a more reliable "crossing-point" scaling technique by extending the 3D XY analysis to finite fields [20]. The subsequent field scaling hypothesis involves the 3D XY scaling variable [2,4]: $x = (H^*/H)^{1/2\nu_{XY}}(T - T_c)/T_c$. The scaling of the ohmic conductivity σ_Ω can then be written as $\sigma_\Omega(H/H^*)^{(z_{XY}-1)/2} = \tilde{s}(x)$, for which the asymptotic behavior is known [4,20]: $\tilde{s}(x) \sim (x + 1)^{-\nu_g(z_g-1)}$ as $x \to -1$, corresponding to $T \to T_g(H)$, and $\tilde{s}(x) \sim x^{-\nu_{XY}(z_{XY}-1)}$ as $x \to +\infty$, corresponding to $H \to 0$.

The crossing-point method proceeds from the definition of x: If $H > 0$ and $T = T_c$, then $x = 0$ and must therefore be independent of H. It follows that, in this limit, $\sigma_\Omega(H/H^*)^{(z_{XY}-1)/2}$ should also be independent of H. Data sets $\sigma_\Omega(T)$, obtained at constant fields H, must then all cross at $T = T_c$ when plotted as in Fig. 2, provided that z_{XY} has been chosen correctly. As observed in the insets, the crossing-point method places strong constraints on the exponent and transition temperature, which we identify as $z_{XY} = 1.25 \pm 0.05$ and $T_c = 60.8 \pm 0.4$, for the film shown. These results are corroborated by low-field data ($H \leq 0.1$ T) [20]. Since 3D XY fluctuations are most prevalent near $T = T_c$, it is helpful to think of this method as optimizing scaling near this temperature. We emphasize that z_{XY} obtained in this way disagrees with the expected [2] diffusive dynamics ($z_{XY} = 2$), and also with other experimental observations [19,21]. It is our opinion that the crossing-point method can achieve better results than those analyses due to the incorporation of finite-field data in the scaling procedure.

The estimates for z_{XY}, ν_{XY}, and T_c, determined above, can be checked through a full scaling analysis of σ_Ω, as shown in Fig. 3. For that film, the initial estimates could not be improved upon. The fitting is excellent at all low fields, becoming optimal at $T = T_c$. For comparison, the best fit, using the expected exponents $z_{XY} = 2$ and $\nu_{XY} = 0.669$, is shown in the inset. As found in previous analyses [4], scaling using $z_{XY} = 2$ suffers at the lowest fields and,

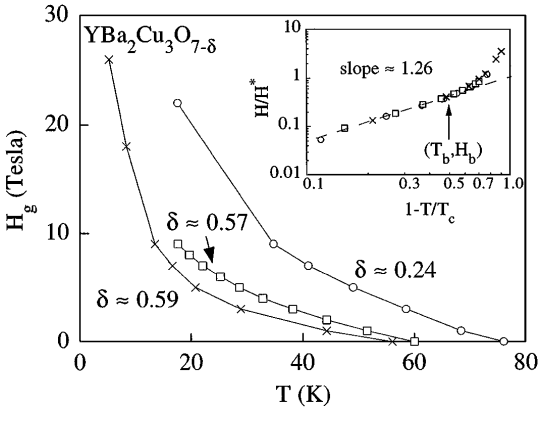

FIG. 1. Superconducting phase boundaries for three deoxygenated $YBa_2Cu_3O_{7-\delta}$ thin films. Lines are a guide to the eye. The inset shows the same phase boundaries plotted logarithmically. Power-law behavior is evident for $H < H_b$.

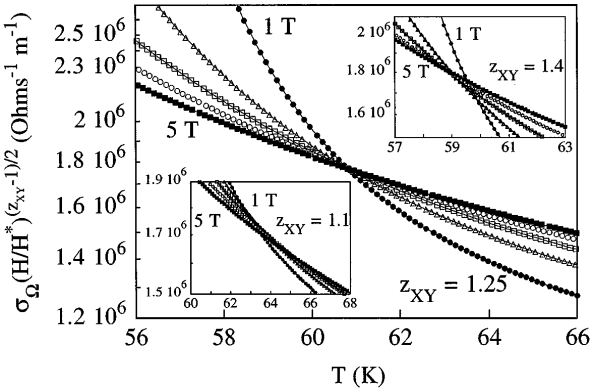

FIG. 2. 3D XY crossing-point method, shown for the $\delta = 0.57$ film. Symbols correspond to different fields: 1, 2, 3, 4, 5 T. The appropriate choice of z_{XY} causes lines to cross at a single point, identifying both z_{XY} and T_c. Poor crossing behavior is observed for (slightly) incorrect values of z_{XY} (insets).

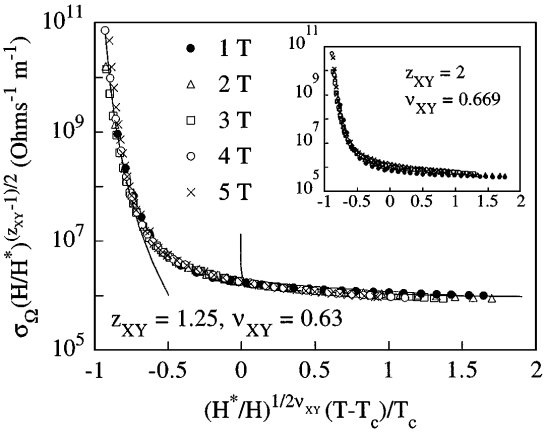

FIG. 3. Full 3D *XY* scaling of the ohmic conductivity σ_Ω for the $\delta \simeq 0.57$ film. Scaling is successful only for low fields ($H < H_b \simeq 5.1$ T). Expected asymptotic behaviors are shown as solid lines. The inset shows the poor scaling obtained using the expected exponents $\nu_{XY} = 0.669$ and $z_{XY} = 2$.

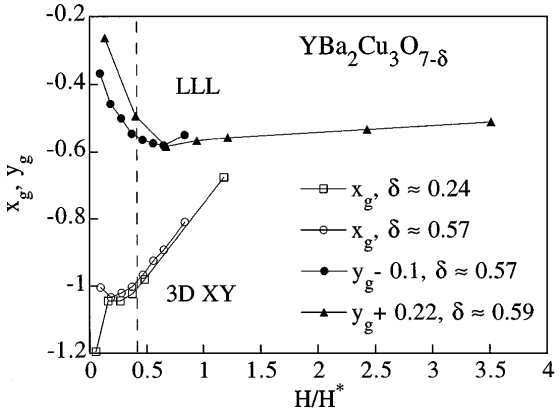

FIG. 4. Multicritical self-consistency: 3D *XY* and LLL scaling parameters x_g and y_g, respectively, evaluated at $T = T_g(H)$. The dashed line indicates the crossover H_b. Scaling variables should remain field independent in their respective scaling regions. For $H < H_b$, 3D *XY* scaling is self-consistent, while for $H > H_b$, LLL scaling is self-consistent.

perhaps more importantly, near T_c. The scaling results found here are therefore an improvement over previous analyses.

The crossover between low- and high-field behavior, observed above using multicritical scaling, can be formulated more conveniently as follows. Since all sample dependence of the 3D *XY* scaling variable x is absorbed into the characteristic field H^*, the divergence of σ_Ω in Fig. 3 must occur at a universal value of $x = -1$ [20]. Multicritical self-consistency therefore requires the scaling variable x_g [i.e., x evaluated along the phase boundary $T_g(H)$] to remain field independent in the 3D *XY* scaling region, as shown in the lower half of Fig. 4. Errors in the determination of x_g are magnified at the lowest fields, where the difference $T_c - T_g(H)$ is small. Deviation from 3D *XY* multicritical self-consistency becomes apparent for $H > H_b$.

Several fluctuation models are candidates for describing the upturn of $H_g(T)$ when $H_g > H_b$ in Fig. 1 (inset). Here, we consider the 3D LLL model, using multicritical theory to place restrictions on the allowable scaling. The scaling technique is constructed in analogy with the preceding 3D *XY* analysis. In the LLL theory, a natural scaling parameter emerges [8,9]: $y = (H^*T_c/HT)^{2/3}[T - T_{c2}(H)]/T_c$, where T_c and H^* have been used here to make y dimensionless. In this analysis it is $T_{c2}(H)$ which must be determined by scaling. Although $T_{c2}(H)$ is often assumed to be linear [8,9], this restriction becomes too severe for the underdoped samples used here. Instead, a LLL crossing-point method is now constructed, which allows the *form* of $T_{c2}(H)$ to be ascertained. As described below, this analysis obtains $T_{c2}(H)$ curves with positive curvature—an interesting feature which has previously been associated only with magnetically doped HTSCs [22].

The LLL crossing-point method is described as follows. We make use of the 3D LLL scaling ansatz [9] which we write as $\sigma_\Omega(HT_c^2/H^*T^2)^{1/3} = F_{3D}(y)$. In analogy with the 3D *XY* case, $\sigma_\Omega(HT_c^2/H^*T^2)^{1/3}$ must be independent of H when $T = T_{c2}(H)$. To begin, a value of T_{c2} is first *assumed* for a particular reference field H_0. The temperatures $T_{c2}(H)$ consistent with this choice are then obtained for other fields ($H \neq H_0$). This is accomplished by plotting $\sigma_\Omega(HT_c^2/H^*T^2)^{1/3}$ vs $T - T_{c2}(H)$ for (fixed H) $\sigma_\Omega(T)$ data sets, then adjusting $T_{c2}(H)$ for each field until a crossing occurs at $T - T_{c2}(H) = 0$, similar to Fig. 2. For fields $H \neq H_0$, $T_{c2}(H)$ is thus a function of the original choice of $T_{c2}(H_0)$, reducing the following fit to a single parameter. All $T_{c2}(H)$ curves found in this way exhibit positive curvature. It is once again helpful to view the crossing point as a method for optimizing scaling in the most essential temperature region; in the LLL case this is near $T_{c2}(H)$.

We are now left with one fitting parameter, $T_{c2}(H_0)$, which cannot be estimated from the crossing-point method alone. The full LLL scaling procedure is now used to determine the single fitting parameter, while simultaneously requiring multicritical self-consistency. In analogy with the 3D *XY* case, this means that the scaling variable y_g [i.e., y evaluated at $T = T_g(H)$] must remain field independent in the LLL scaling region. We find that, by using $T_{c2}(H)$ obtained from the crossing-point method, multicritical self-consistency *cannot be met at low fields*. Since the LLL theory has its greatest justification at high fields, we attempt, instead, to obtain self-consistency in the high-field region. The outcome of the final scaling procedure is shown in Fig. 5. The (approximate) field independence of y_g is evident for the entire high-field range $H > H_b$, as shown in the top half of Fig. 4. $T_{c2}(H)$ is obtained with only small uncertainty, as shown in Fig. 5 (inset).

We comment finally on the difference between the present results and those of Refs. [10,13]. In our work, LLL scaling is found to be multicritically self-consistent only at

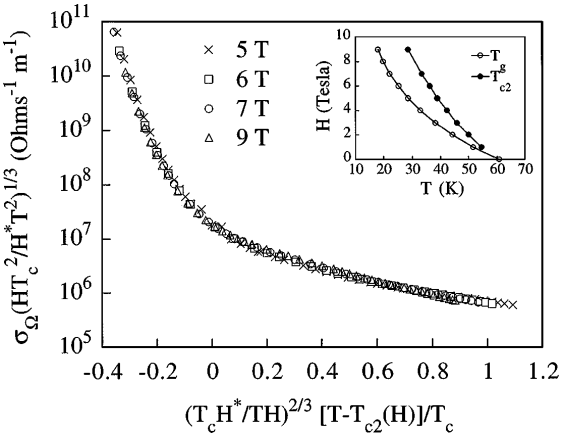

FIG. 5. Full LLL scaling of σ_Ω for the $\delta \simeq 0.57$ film. Multicritically self-consistent scaling is successful only for high fields ($H > H_b \simeq 5.1$ T). The inset shows $T_{c2}(H)$ and $T_g(H)$ for the same film. [$T_{c2}(H)$ is speculative for $H < H_b$.]

high fields ($H > H_b$), while Refs. [10,13], which do not check for self-consistency, find that LLL scaling is applicable at low fields ($H < H_b$). (Note that H_b is very large in the optimal samples used by those authors.) We speculate that scaling could be accomplished in Refs. [10,13] only by allowing diminished scaling quality in precisely the region where the quality should be highest [i.e., near $T_{c2}(H)$]. In the present work, this situation is avoided by optimizing scaling near $T_{c2}(H)$ from the outset.

After the completion of this work, we learned of similar 3D XY results, obtaining $z_{XY} \lesssim 2$ from conductivity scaling [23].

We thank S. Girvin, A. MacDonald, S. Pierson, Z. Tešanović, and especially P. Muzikar for many helpful discussions. This work was supported through the Midwest Superconductivity Consortium (MISCON) DOE Grant No. DE-FG02-90ER45427, the Materials Research Science and Engineering Center (MRSEC) Program of the NSF under Award No. DMR-9400415, and the National High Magnetic Field Laboratory (Tallahassee).

[1] I. D. Lawrie, Phys. Rev. B **50**, 9456 (1994).
[2] M. P. A. Fisher, Phys. Rev. Lett. **62**, 1415 (1989); D. S. Fisher *et al.*, Phys. Rev. B **43**, 130 (1991).
[3] S. E. Inderhees *et al.*, Phys. Rev. Lett. **66**, 232 (1991); G. Mozurkewich *et al.*, Phys. Rev. B **46**, 11 914 (1992); N. Overend *et al.*, Phys. Rev. Lett. **72**, 3238 (1994); M. A. Howson *et al.*, Phys. Rev. Lett. **74**, 1888 (1995); N. Overend *et al.*, Phys. Rev. Lett. **75**, 1870 (1995).
[4] M. B. Salamon *et al.*, Phys. Rev. B **47**, 5520 (1993); M. B. Salamon *et al.*, Physica (Amsterdam) **200A**, 365 (1993).
[5] M. A. Hubbard *et al.*, Physica (Amsterdam) **259C**, 309 (1996).
[6] S. Kamal *et al.*, Phys. Rev. Lett. **73**, 1845 (1994); S. M. Anlage *et al.*, Phys. Rev. B **53**, 2792 (1996); note also the counterexample of Z.-H. Lin *et al.*, Europhys. Lett. **32**, 573 (1995).
[7] N.-C. Yeh *et al.*, Phys. Rev. B **47**, 6146 (1993); M. A. Howson *et al.*, Phys. Rev. B **51**, 11 984 (1995).
[8] A. J. Bray, Phys. Rev. B **9**, 4752 (1974); D. J. Thouless, Phys. Rev. Lett. **34**, 946 (1975); G. J. Ruggeri and D. J. Thouless, J. Phys. F **6**, 2063 (1976); R. Ikeda *et al.*, J. Phys. Soc. Jpn. **58**, 1377 (1989); S. Hikami and A. Fujita, Phys. Rev. B **41**, 6379 (1990).
[9] S. Ullah and A. T. Dorsey, Phys. Rev. Lett. **65**, 2066 (1990); Phys. Rev. B **44**, 262 (1991).
[10] U. Welp *et al.*, Phys. Rev. Lett. **67**, 3180 (1991).
[11] B. Zhou *et al.*, Phys. Rev. B **47**, 11 631 (1993); A. Junod *et al.*, Physica (Amsterdam) **211C**, 304 (1993); S. W. Pierson *et al.*, Phys. Rev. Lett. **74**, 1887 (1995); M. Roulin *et al.*, Phys. Rev. Lett. **75**, 1869 (1995); M. Roulin *et al.*, Physica (Amsterdam) **244C**, 225 (1995); S. W. Pierson *et al.*, Phys. Rev. B **53**, 8638 (1996).
[12] O. Jeandupeux *et al.*, Phys. Rev. B **53**, 12 475 (1996).
[13] D. H. Kim *et al.*, Phys. Rev. B **45**, 10 801 (1992).
[14] Z. Tešanović, Phys. Rev. B **51**, 16 204 (1995).
[15] L. Hou *et al.*, Phys. Rev. B **50**, 7226 (1994).
[16] J. C. LeGuillou and J. Zinn-Justin, J. Phys. (Paris) **46**, L137 (1985).
[17] J. Deak *et al.*, Phys. Rev. B **51**, 705 (1995).
[18] A. Schilling *et al.*, Phys. Rev. Lett. **71**, 1899 (1993); C. C. Almasan and B. Maple, Phys. Rev. B **53**, 2882 (1996); K. Kishio, in *Physical Properties of High Temperature Superconductors*, edited by D. M. Ginsberg (World Scientific, Singapore, 1996).
[19] J. M. Roberts *et al.*, Phys. Rev. B **49**, 6890 (1994).
[20] M. Friesen *et al.* (unpublished).
[21] J. C. Booth *et al.*, Phys. Rev. Lett. **77**, 4438 (1996).
[22] Yu. N. Ovchinnikov and V. Z. Kresin, Phys. Rev. B **54**, 1251 (1996), and references therein.
[23] D. Ginsberg, J.-T. Kim, and N. Goldenfeld (unpublished).